COMPOSITE MODELING CAPABILITIES OF COMMERCIAL FINITE ELEMENT SOFTWARE

Thesis

Presented in the Partial Fulfillment of the Requirements for the Graduation with Distinction in the Undergraduate School of Engineering at The Ohio State University

By

Brice Matthew Willis

Undergraduate Program in Aerospace Engineering

The Ohio State University

2012

Thesis Committee

Dr. Rebecca Dupaix, Advisor

Dr. Mark Walter

Abstract

Carbon fiber reinforced polymers (CFRPs) can match or exceed the stiffness properties of steel or aluminum with nearly half the weight. Therefore, the desire to replace steel and aluminum is growing in order to make more fuel efficient vehicles. One drawback of CFRPs is that they require more complex techniques to model them in commercial finite element software. Two software packages that are widely used in industry are ANSYS and Abaqus, therefore, techniques to model composites need to be investigated using each of these software packages. To determine their abilities, a tension test of a CFRP coupon will be constructed. The coupon will be a 2 inch by 5 inch composite laminate that will be modeled with three different lay-up patterns. The modeled specimens will be subjected to a 5000 pound force in the global y direction. FEA solutions returned from ANSYS and Abaqus are then compared to each other and verified using current laminate theory. Following the verification, the discussed modeling techniques will be applied to more complex geometries, such as a holed specimen and a notched specimen. The modeling techniques add to the knowledge base of composite modeling and show how results from ANSYS and Abaqus compare to each other.

Acknowledgements

I would like to thank Dr. Walter and Dr. Dupaix for the time that they have spent advising the carbon fiber research team at The Ohio State University.

I would also like to thank Brooks Marquette and Hisham Sawan for being excellent team members of the carbon fiber research team.

Vita

2007 to present…….....Department of Mechanical and Aerospace Engineering

The Ohio State University.

Fields of Study

Major Field:

Bachelor of Science in Aeronautical and Astronautical Engineering

Table of Contents

List of Figures

List of Tables

1. Introduction

The definition of a composite material is very flexible, but in the most general terms it is a material that is composed of two or more distinct constituents. The use of composite materials in engineering applications dates back to the ancient Egyptians and their use of straw in clay to construct buildings (Swanson, 1997). In modern times composites have been used in civil engineering applications, aerospace engineering applications, and many places in between. For example, the automotive industry introduced large-scale use of composites with the Chevrolet Corvette (Staab, 1999). The relative importance of composite development compared to other engineering materials can be seen in Figure 1.

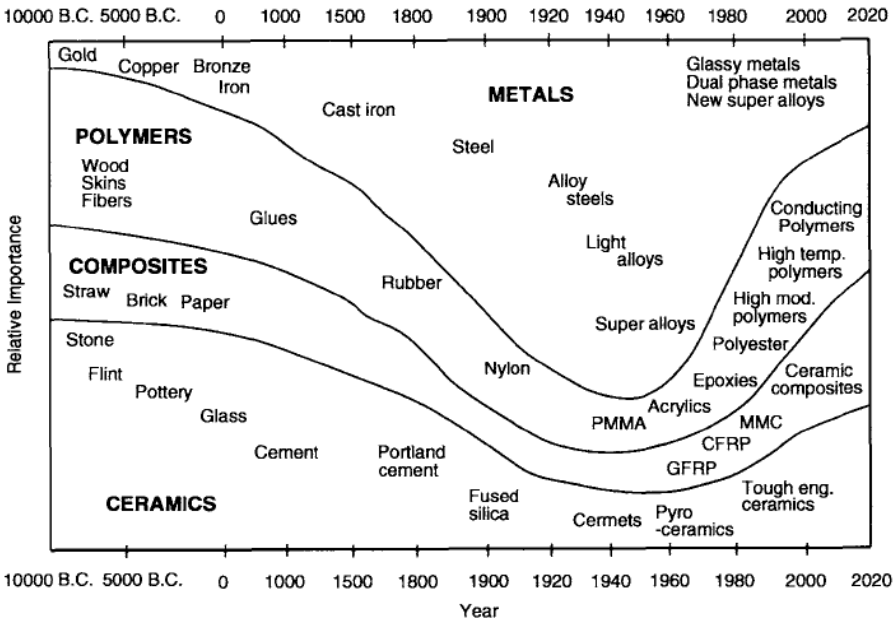

Figure 1: Relative importance of material development through history (Staab, 1999)

Automotive applications of composite materials, particularly carbon fiber reinforced polymers (CFRPs), began with high performance vehicles. CFRPs were used to replace body panels, floor panels, wheel housings, and hoods. This was done to reduce the weight of these vehicles in

order to increase their acceleration and speed on the race track. The high cost of CFRPs has limited their use to high performance and racing vehicles. The increase in fuel costs and the growing movement to reduce harmful emissions is pushing automobile companies to reduce the weight of their vehicles in order to increase the fuel economy. A 10 percent reduction of vehicle mass can increase a vehicles gas mileage by up to 7 percent (Unknown, 2008). Therefore, the high strength-to-weight ratios of CFRPs is being sought to decrease the weight of the common vehicle. A comparison of the strength-to-weight ratio properties of CFRPs to other materials can be seen in Figure 2 and Figure 3.

Replacing car parts with CFRPs poses some problems to engineers. CFRP components are not as simple to model as traditional engineering materials (steel, aluminum, etc.). First of all, composite materials generally do not behave in an isotropic manner. Composite materials, such as CFRPs, behave in an anisotropic or orthotropic manor. Anisotropic and orthotropic mechanical behaviors are difficult to predict compared to isotropic behaviors. Therefore, finite element analysis (FEA) packages must use more complex material models to predict these behaviors. High performance composite components are made by bonding multiple plies of unidirectional plies into a 3D laminate part.

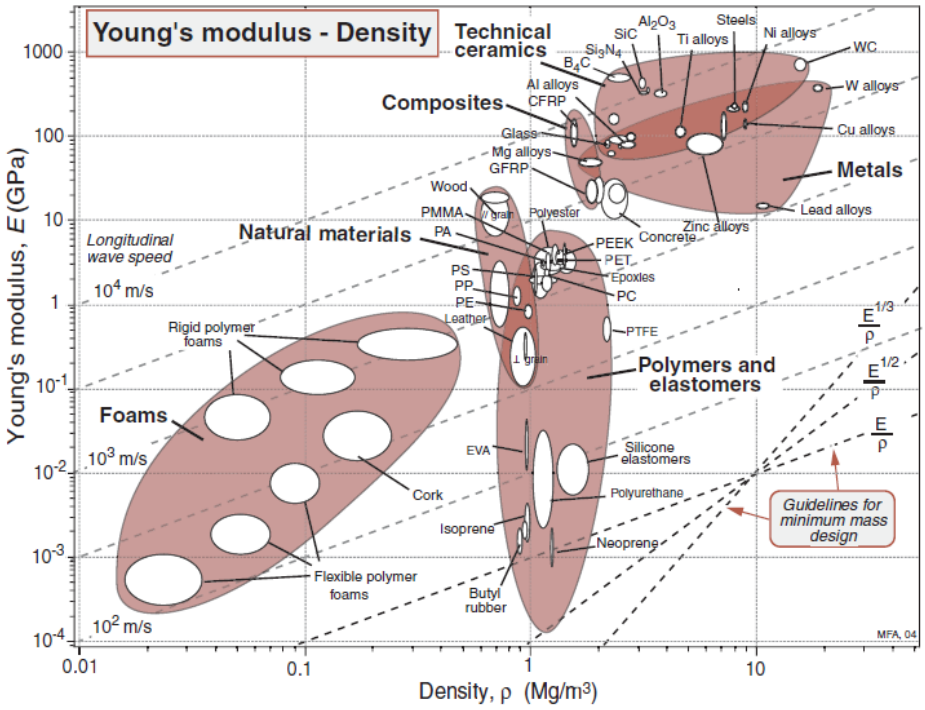

Figure 2: Envelopes comparing the Young's modulus, E, vs. density, ρ, of various engineering materials (Ashby, 2005)

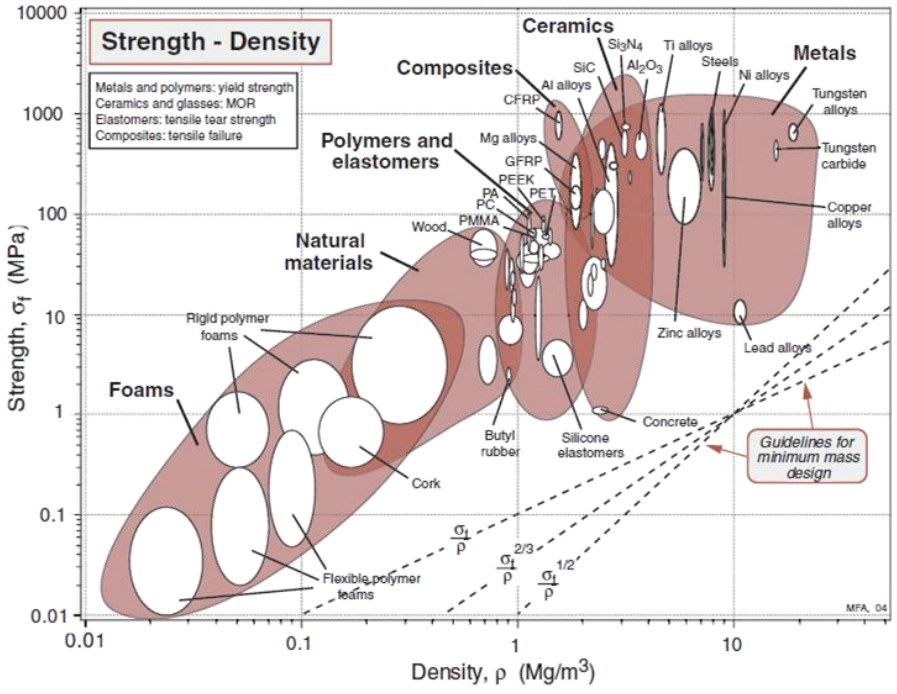

Figure 3: Envelopes comparing the strength, σ_f, vs. density, ρ, of various engineering materials (Ashby, 2005)

1.1 Focus of Thesis

The finite element method (FEM) is used to predict multiple types of static and dynamic structural responses. For example, companies in the automotive industry use it to predict, stress, strain, deformations, and failure of many different types of components. FEA reduces the need for costly experiments and allows engineers to optimize parts before they are built and implemented. There are many software packages available to industries that use FEA. A list of some of these commercial packages can be seen in Table 1.

Table 1: Commercially available FEA software (Miracle & Donaldson, 2001)

Code	Company	Web address
Codes with built-in pre- and postprocessors for composites		
ABAQUS	Hibbitt, Karlsson & Sorensen, Inc., Pawtucket, RI	http://www.abaqus.com/products/
ALGOR	Algor, Inc., Pittsburgh, PA	http://algor.com/homepag2.htm
ANSYS	ANSYS, Inc., Canonsburg, PA	http://www.ansys.com/
CATIA/Elfini	IBM and Dessault Systemes, Newark, NJ	http://www.catia.ibm.com/prodinfo/cov.html
COSMOS	Structural Research & Analysis Corp., Los Angeles, CA	http://www.srac.com/products.html
EMRC-NISA II	Engineering Mechanics Research Corp., Troy, MI	http://www.emrc.com/webpages/composite/compov.html
ESI-SYSPLY	ESI Group, Paris, France	http://www.esi.fr/products/sysply/overview.html
ESRD-StressCheck	Engineering Software Research and Development, Inc., St. Louis, MO	http://www.esrd.com/CompositeAnalysis.htm
Pro/MECHANICA	PTC, Needham, MA	http://www.ptc.com/products/proe/sim/structural.htm
SDRC-IDEAS	Structural Dynamics Research Corp., Milford, OH	http://www.sdrc.com/nav/software-services/product-catalog/lamcomp.pdf
Codes using separate pre- and postprocessors		
LS-DYNA	Livermore Software Technology Corporation, Livermore, CA	http://www.lstc.com
MSC-NASTRAN/DYTRAN	MSC Software Corp., Costa Mesa, CA	http://www.mechsolutions.com/products/patran/lammod.html
VR&D-GENESIS	Vanderplaats Research & Development, Inc., Colorado Springs, CO	http://www.vrand.com/genesis_fact.htm
Pre- and postprocessors		
PATRAN	MSC Software Corp., Costa Mesa, CA	http://www.mechsolutions.com/products/patran/patran2000.htm
HyperMesh	Altair Engineering, Inc., Troy, MI	http://www.altair.com/

The focus of the thesis is to compare the composite analysis abilities of ANSYS and Abaqus. The comparison will be completed by modeling composite laminates of different orientations. Out of the packages listed above, ANSYS and Abaqus were selected due to their availability at The Ohio State University and their wide usage in industry and research.

1.2 Significance of Research

Composite materials have very different structural responses than traditional materials. This is mainly due to their anisotropic and orthotropic elastic behavior. Therefore, for an engineer to properly design a composite he/she must understand how to construct a model in FEA software. A fundamental understanding of composite modeling will allow engineers to design car parts that match or exceed the performance of steel or aluminum parts. The stronger and lighter parts will lead to safer more fuel efficient vehicles. This research will provide insight on the differences between ANSYS and Abaqus along with a fundamental understanding of creating composite models.

1.3 Overview of Thesis

This thesis has 5 chapters. Chapter 2 consists of a discussion on the theory behind lamina analysis. The theoretical discussion will focus on the theory used to construct a MATLAB code used to verify the FEA results. Chapter 3 will discuss the setup of the FEA models in ANSYS and Abaqus. It will discuss the tests that were modeled, the material models used, element types, and the unique attributes of each FEA package. The results from the simulations and theoretical calculations will be compared to each other in Chapter 4. ANSYS will then be used to simulate a holed and notched tension specimen in chapter 5. Then in the final chapter conclusions will be drawn, contributions will be discussed, applications will be described, and future work will be proposed. The thesis will also be briefly summarized in order to reiterate the big picture of the research.

2. Laminate Analysis

Laminated composite materials are much more difficult to analyze compared to traditional materials. This is due to the fact that the mechanical response of a composite material is dependent on the direction of loading and they tend to react in an anisotropic or orthotropic manner. In order to analyze the mechanical response of a laminate, the behavior of each individual ply must be predicted (Staab, 1999). To do so, assumptions were made and theories were derived.

The first assumption is that the material is perfect. For a laminate, in this context, perfect describes a ply that is free of defects, a single ply consists of a single layer of fibers, and that the fiber arrangement is uniform. A simple depiction of the fiber distribution in an actual ply compared to the modeled ply can be seen in Figure 4. The perfect arrangement of fibers also allows the material to be modeled as an orthotropic material.

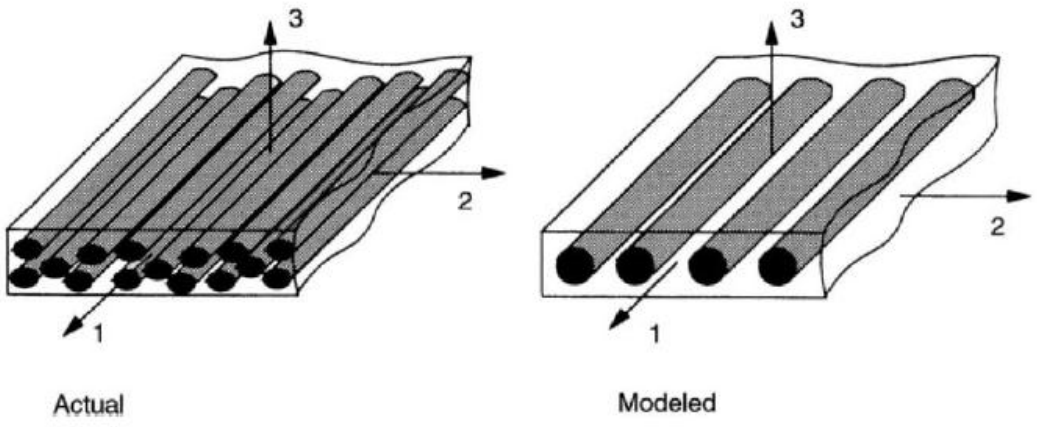

Figure 4: Schematic of actual and modeled lamina (Staab, 1999)

Laminate theories were used in order to validate tension tests simulated using FEA. These theories calculate the stress across the thickness of each ply of the laminate. The theory will be discussed in the following text.

2.1 Theoretical laminate analysis

For the discussion subscripts 1, 2, and 3 will represent principal fiber direction, in-plane direction perpendicular to the fibers, and out-of-plane direction perpendicular to the fibers. These numbers also represent the principal axes of the orthotropic material behavior. These axes can also be seen in Figure 4.

For the analysis throughout this section the lamina will be analyzed using plane stress conditions. Assuming plane stress conditions reduces the level of complexity of the analysis because the model is reduced from three dimensional to two dimensional. Therefore, this analysis is only concerned with the material properties in principal directions 1 and 2. To predict the axial stress in a lamina E_1, E_2, G_{12}, and v_{12} must be provided for the material in question. The number of plies, their thickness, width, and orientation must also be provided.

To initiate the stress calculations, the provided material properties can be used to calculate v_{21}. This Poisson's ratio was calculated using the following equation (Staab, 1999).

$$v_{21} = v_{12}\frac{E_2}{E_1}$$

The provided moduli and Poisson's ratios can be used to construct a stiffness matrix. The stiffness matrix for plane stress conditions can be seen in the matrix below (Staab, 1999).

$$[Q] = \begin{bmatrix} Q_{11} & Q_{12} & 0 \\ Q_{12} & Q_{22} & 0 \\ 0 & 0 & Q_{66} \end{bmatrix}$$

In this matrix the individual terms are

$$Q_{11} = \frac{E_1}{1 - v_{12}v_{21}}$$

$$Q_{22} = \frac{E_2}{1 - v_{12}v_{21}}$$

$$Q_{12} = \frac{v_{12}E_2}{1 - v_{12}v_{21}} = \frac{v_{21}E_1}{1 - v_{12}v_{21}}$$

$$Q_{66} = G_{12}$$

This stiffness matrix was calculated for each ply of the lamina. The matrix was constructed relative to the orientation of each individual ply. The orientation of the fibers in each ply as they relate to the global coordinate system can be seen in Figure 5.

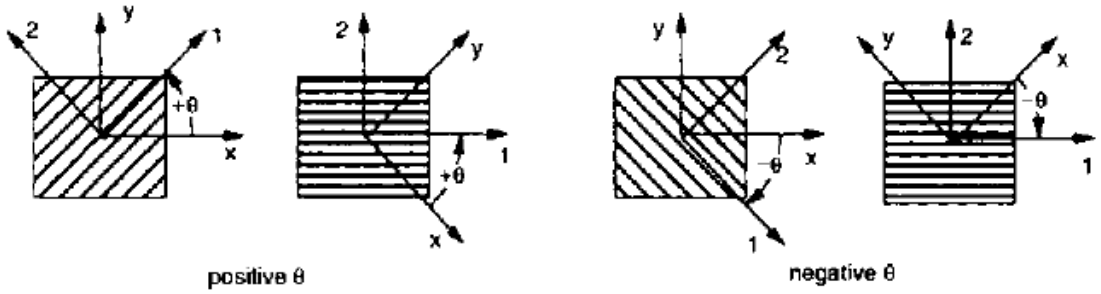

Figure 5: Sign convention of positive and negative fiber orientations (Staab, 1999)

The stiffness matrix for each of the plies has to be transformed into the global coordinate system in order to obtain the stresses in the global directions. This transformation will formulate a new stiffness matrix, seen below (Staab, 1999).

$$[\bar{Q}] = \begin{bmatrix} \bar{Q}_{11} & \bar{Q}_{12} & \bar{Q}_{16} \\ \bar{Q}_{12} & \bar{Q}_{22} & \bar{Q}_{26} \\ \bar{Q}_{16} & \bar{Q}_{26} & \bar{Q}_{66} \end{bmatrix}$$

In the converted stiffness matrix the individual terms are ($m = cos\theta, n = sin\theta$)

$$\bar{Q}_{11} = Q_{11}m^4 + 2(Q_{12} + 2Q_{66})m^2n^2 + Q_{22}n^4$$

$$\bar{Q}_{12} = (Q_{11} + Q_{22} - 4Q_{66})m^2n^2 + Q_{12}(m^4 + n^4)$$

$$\bar{Q}_{16} = -Q_{22}mn^3 + Q_{11}m^3n - (Q_{12} + 2Q_{66})mn(m^2 - n^2)$$

$$\bar{Q}_{22} = Q_{11}n^4 + 2(Q_{12} + 2Q_{66})m^2n^2 + Q_{22}m^4$$

$$\bar{Q}_{26} = -Q_{22}nm^3 + Q_{11}n^3m - (Q_{12} + 2Q_{66})mn(m^2 - n^2)$$

$$\bar{Q}_{66} = (Q_{11} + Q_{22} - 2Q_{12})m^2n^2 + Q_{66}(m^2 - n^2)$$

The $[\bar{Q}]$ matrices for each of the different plies are then added together. This summed matrix will be represented by $[\bar{Q}]_{total}$. The total matrix can be used to predict the strain that is caused by an applied tensile stress. This calculation can be seen in the equation below.

$$\begin{bmatrix} \varepsilon_1 \\ \varepsilon_2 \\ \varepsilon_6 \end{bmatrix} = [\bar{Q}]_{total}^{-1} \begin{bmatrix} N_1 \\ N_2 \\ N_3 \end{bmatrix}$$

The stress throughout the lamina can then be predicted using the following relation (Staab, 1999).

$$\begin{Bmatrix} \sigma_x \\ \sigma_y \\ \sigma_{xy} \end{Bmatrix} = \begin{bmatrix} \bar{Q}_{11} & \bar{Q}_{12} & \bar{Q}_{16} \\ \bar{Q}_{12} & \bar{Q}_{22} & \bar{Q}_{26} \\ \bar{Q}_{16} & \bar{Q}_{26} & \bar{Q}_{66} \end{bmatrix} \begin{Bmatrix} \varepsilon_1 \\ \varepsilon_2 \\ \varepsilon_6 \end{Bmatrix}$$

2.2 Laminate analysis using ANSYS

Within ANSYS there are many different elements that can be used to model composite lay ups. The element types used by ANSYS are referred to as finite strain shell elements, 3D layered structural solid shell elements, and 3D layered structural solid elements. There are a variety of specific elements associated with each element type. Specific element selection depends upon application and the type of results that must be calculated (Anonymous_2, 2009). Different finite strain shell elements can be chosen depending on the number of composite layers, the thickness of each layer, and the expected magnitude of the displacements/rotations of the model. Selection of 3D layered structural solid elements is based upon the geometry of the structure being modeled. Structures with through the thickness discontinuities or that have a wide range of shell thicknesses within the part should be modeled using 3D layered structural shell elements. The most complex of the previously stated element types is the 3D layered structural element. This element type should be selected to model exotic 3D geometries. This element type should also be selected if information about plasticity, hyperelasticity, stress stiffening, creep, large deflections, and large strains is desired. A list of specific elements and their elements types can be seen in Table 2.

Table 2: ANSYS elements that can be used for composite analysis (Anonymous_2, 2009)

Element Name	Element Type	Description
SHELL181	Finite Strain Shell	A 4-node 3-D shell element with 6 degrees of freedom at each node. The element has full nonlinear capabilities including large strain and allows 255 layers.
SHELL281	Finite Strain Shell	An 8-node element with six degrees of freedom at each node. The element is suitable for analyzing thin to moderately-thick shell structures and is appropriate for linear, large rotation, and/or large strain nonlinear applications.
SOLSH190	3-D Layered Structural Solid Shell	An 8-node 3-D solid shell element with three degrees of freedom per node (UX, UY, UZ). The element can be used for simulating shell structures with a wide range of thickness (from thin to moderately thick). The element has full nonlinear capabilities including large strain and allows 250 layers for modeling laminated shells.
SOLID185	3-D Layered Structural Solid Element	A 3-D 8-Node Layered Solid used for 3-D modeling of solid structures. It is defined by eight nodes having three degrees of freedom at each node: translations in the nodal x, y, and z directions. The element has plasticity, hyperelasticity, stress stiffening, creep, large deflection, and large strain capabilities. It also has mixed formulation capability for simulating deformations of nearly incompressible elastoplastic materials, and fully incompressible hyperelastic materials. The element allows for prism and tetrahedral degenerations when used in irregular regions.
SHELL63	Shell	This 4-node shell element can be used for rough, approximate studies of sandwich shell models. A typical application would be a polymer between two metal plates, where the bending stiffness of the polymer would be small relative to the bending stiffness of the metal plates. The bending stiffness can be adjusted by the real constant RMI to represent the bending stiffness due to the metal plates, and distances from the middle surface to extreme fibers (real constants CTOP, CBOT) can be used to obtain output stress estimates on the outer surfaces of the sandwich shell.

2.3 Laminate analysis using Abaqus

As mentioned earlier, the Abaqus FEA package also provides built in composite modeling capabilities. Abaqus allows the user to define composite layups for three types of elements. These element types are referred to as continuum shell elements, conventional shell elements, and solid elements. Abaqus also has an extensive list of solid 3-D elements that are described in chapter 23.1.4 of the Abaqus documentation. When analyzing composites the Abaqus user should only use solid elements when the transverse shear effects are predominant, when the normal stress cannot be ignored, and when accurate interlamintate stresses are desired. Like ANSYS, the type of element that should be used to model a component is based on the component's geometry and the results desired. The element type selection process in Abaqus follows the same criterion as ANSYS. Like ANSYS, Abaqus offers a GUI that is used to define

the properties of a layered composite structure. This GUI is referred to as the composite layup editor. The composite layup editor provides a table that the user can use to define the plies in the layup (Anonymous, 2008). This table can be used to assign a name, material, thickness, and orientation to each ply. The ply table also provides several options that make it easier for the user to create a layered composite containing many plies. These options include; the ability to move or copy selected plies up or down in the table, suppress or delete plies, create patterns with a group of selected plies, and read ply data from or write data to an ASCII file. The ability to suppress plies allows the user to easily experiment with different configurations of plies in the composite layup and see the effect on the results of an analysis of a model (Anonymous, 2008). A list the element types and specific elements names used by Abaqus to analyze composites can be seen in Table 3.

Table 3: ANSYS elements that can be used for composite analysis (Anonymous, 2008)

Element Name	Element Type	Description
STRI3$^{(S)}$	Conventional Shell	3-node triangular facet thin shell
S3	Conventional Shell	3-node triangular general-purpose shell, finite membrane strains (identical to element S3R)
S3R	Conventional Shell	3-node triangular general-purpose shell, finite membrane strains (identical to element S3)
S3RS$^{(E)}$	Conventional Shell	3-node triangular shell, small membrane strains
STRI65$^{(S)}$	Conventional Shell	6-node triangular thin shell, using five degrees of freedom per node
S4	Conventional Shell	4-node doubly curved general-purpose shell, finite membrane strains
S4R	Conventional Shell	4-node doubly curved general-purpose shell, reduced integration with hourglass control, finite membrane strains
S4RS$^{(E)}$	Conventional Shell	4-node, reduced integration, doubly curved shell with hourglass control, small membrane strains
S4RSW$^{(E)}$	Conventional Shell	4-node, reduced integration, doubly curved shell with hourglass control, small membrane strains, warping considered in small-strain formulation
S4R5$^{(S)}$	Conventional Shell	4-node doubly curved thin shell, reduced integration with hourglass control, using five degrees of freedom per node
S8R$^{(S)}$	Conventional Shell	8-node doubly curved thick shell, reduced integration
S8R5$^{(S)}$	Conventional Shell	8-node doubly curved thin shell, reduced integration, using five degrees of freedom per node
S9R5$^{(S)}$	Conventional Shell	9-node doubly curved thin shell, reduced integration, using five degrees of freedom per node
SC6R	Continuum Shell	6-node triangular in-plane continuum shell wedge, general-purpose, finite membrane strains
SC8R	Continuum Shell	8-node hexahedron, general-purpose, finite membrane strains

3 Modeling

The mechanical behavior of laminates was investigated using ANSYS (Canonsburg, PA, USA) and Abaqus (Providence, RI, USA). In each of these packages 3 laminates of different orientations were modeled. The orientations in question are unidirectional, quasi-isotropic, and cross-ply. All of these laminates consisted of seven 0.005 inch thick plies of the same material. The layers modeled were intended to simulate a carbon fiber reinforced impregnated tape. A unidirectional orientation can be seen in Figure 6, followed by a quasi-isotropic orientation in Figure 7 and a cross-ply in Figure 8.

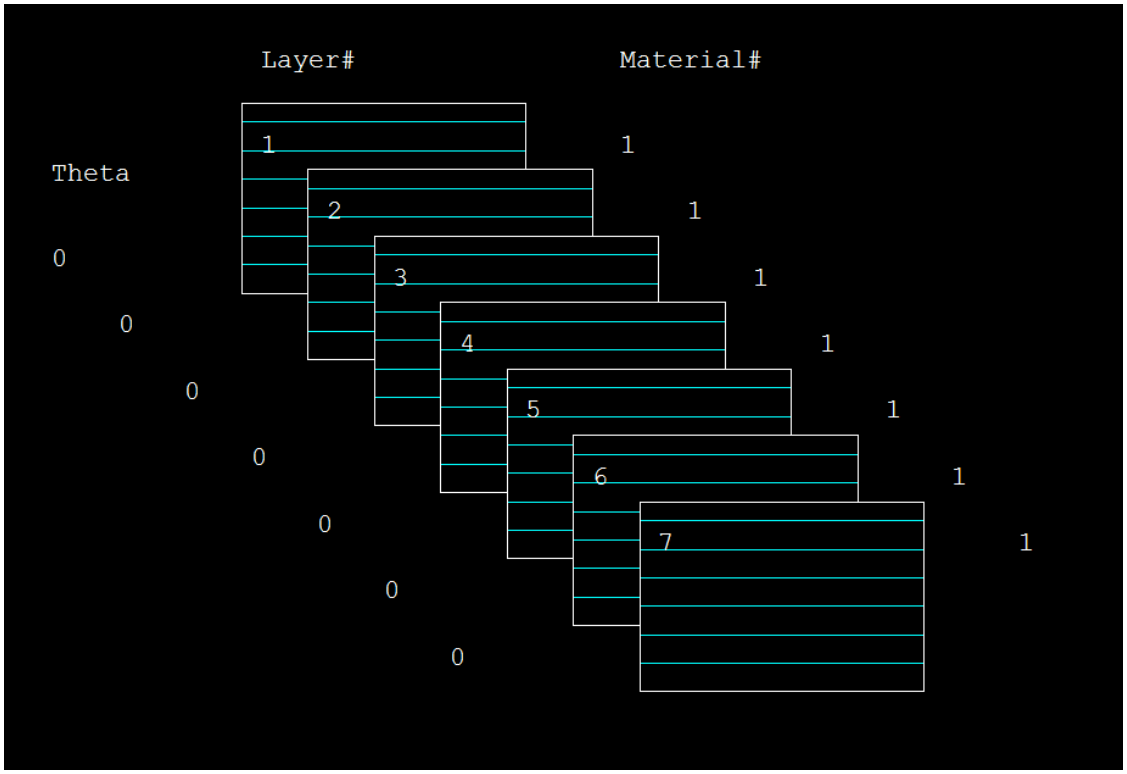

Figure 6: Unidirectional lay-up

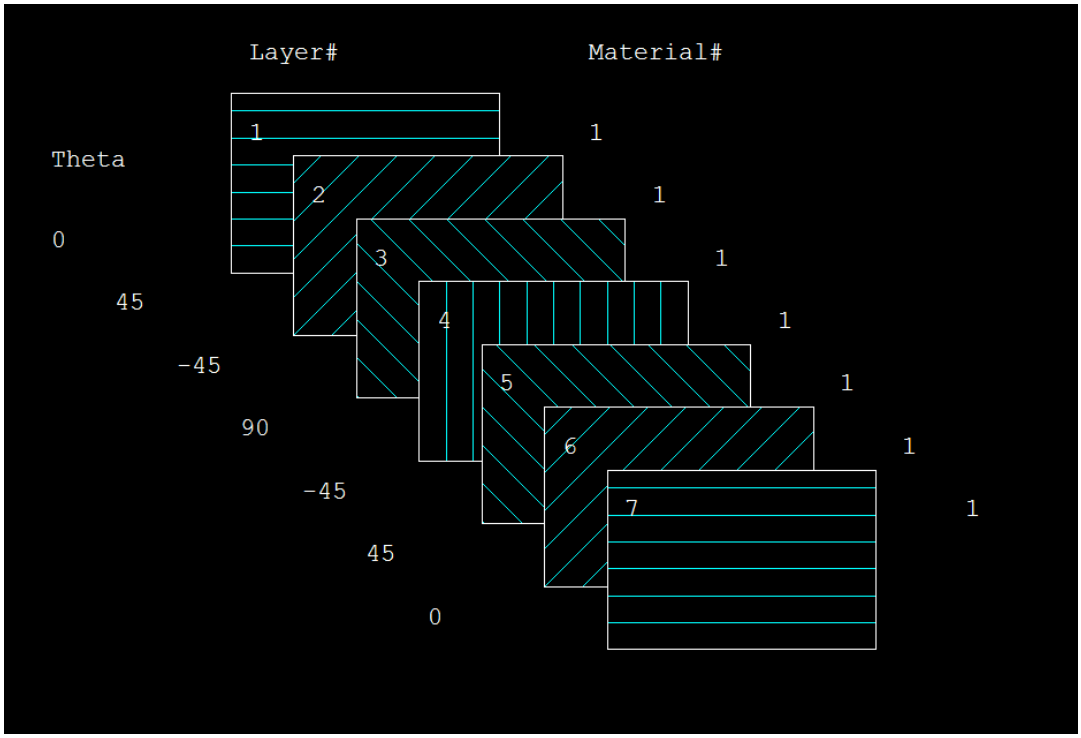

Figure 7: Quasi-isotropic lay-up

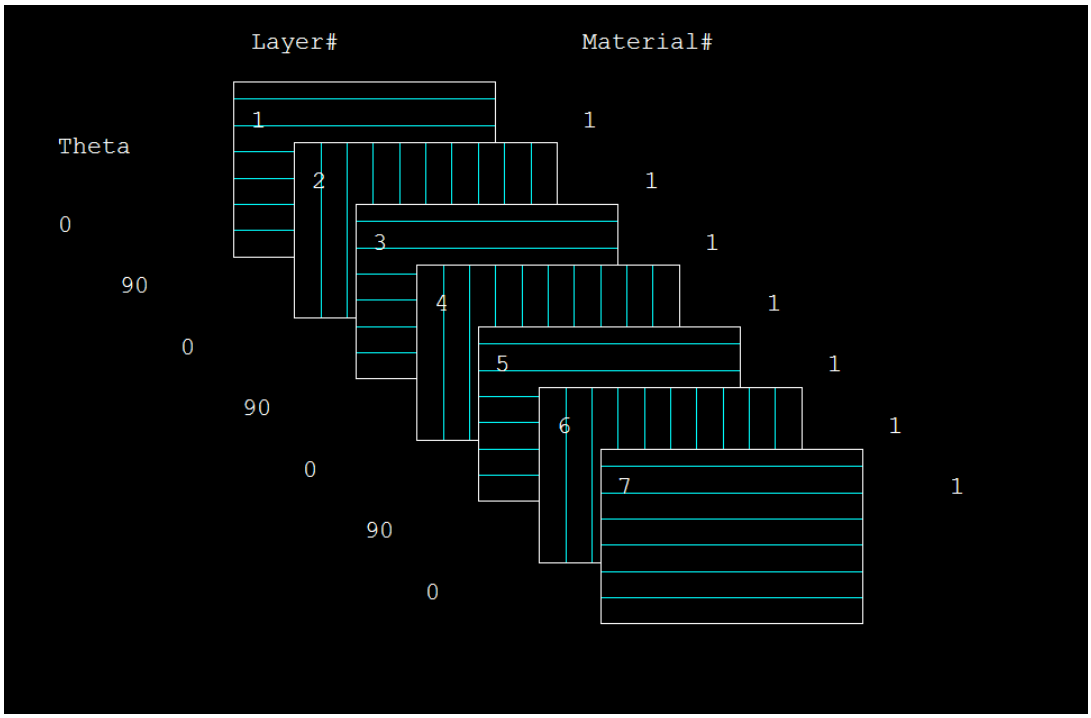

Figure 8: Cross-ply lay-up

Material properties for each ply were prescribed using the properties in Table 4. This type of carbon-fiber composite has a modulus that is roughly 12 times stiffer in the direction of the fibers than transverse to the fibers. Also, the anisotropy effects are less important in shear/Poisson's ratio. These two phenomena are due to the fact that the fibers are much stiffer than the surrounding matrix.

Table 4: Elastic properties of each ply (Feraboli & Kedward, 2003)

$E_x = 18$ Msi (124.1 GPa)	$E_y = 1.5$ Msi (10.3 GPa)	$E_z = 1.5$ Msi (10.3 GPa)
$G_{xy} = 0.8$ Msi (55.2 GPa)	$G_{xz} = 0.8$ Msi (55.2 GPa)	$G_{yz} = 0.6$ Msi (4.1 GPa)
$\nu_{xy} = 0.3$	$\nu_{xz} = 0.3$	$\nu_{yz} = 0.35$

3.1 Meshing and boundary conditions

Tension tests were simulated in ANSYS and Abaqus in order to examine the stresses throughout the thickness of the laminate. In each of the packages the laminate was meshed as using shell elements. The specific element used in ANSYS is referred to as SHELL281 and the shell element in Abaqus is known as S8R. Each of these elements are 8-node (quadratic) quadrilaterals. Also, each node of these elements has six degrees of freedom. The shell elements were prescribed section properties using the lay-up editors available in both FEA packages. The model geometry consisted of a rectangular plate 2 inches wide by 5 inches tall. The element edge sizing was set to 0.25 inch, giving a 20 x 8 mesh consisting of 160 elements. This mesh size was arbitrarily selected based on previous FEA experience. Since the FEA results matched the theoretical results, the mesh sizing was not adjusted. It is likely that the mesh size could be significantly reduced while still obtaining the same results. The model could

have also been simplified by applying quarter symmetry. Since computational cost wasn't an issue for this test the selected mesh size wasn't adjusted and the entire tension specimen was modeled. For more complex models, where computational cost maybe an issue, it would be useful to apply any simplifications that can be justified.

For the simulation the bottom edge of the test coupon was constrained and a force was applied to the top edge. The line on the bottom of the shell was constrained in the y-direction. Also, to allow for Poisson's effects and to prevent rigid body motion, the node at the bottom corner was constrained in all degrees of freedom. The force was prescribed to be distributed evenly across the top edge of the shell. To simulate a total force of 5000 pounds, an edge pressure of 2500 pounds per inch had to be prescribed. This model is an idealization of a tension test. In reality the grips used to hold the tension coupon would apply more of a constraint in the x direction, which would cause the stress near the edge of the part to be non-uniform. These effects can be accounted for by making the tension specimen taller. This is justified by Saint-Venant's principle. Also, since the constraints in the model are perfect, the height of the specimen doesn't affect the FEA solution. An illustration of the previously described boundary conditions and forces can be seen in Figure 9.

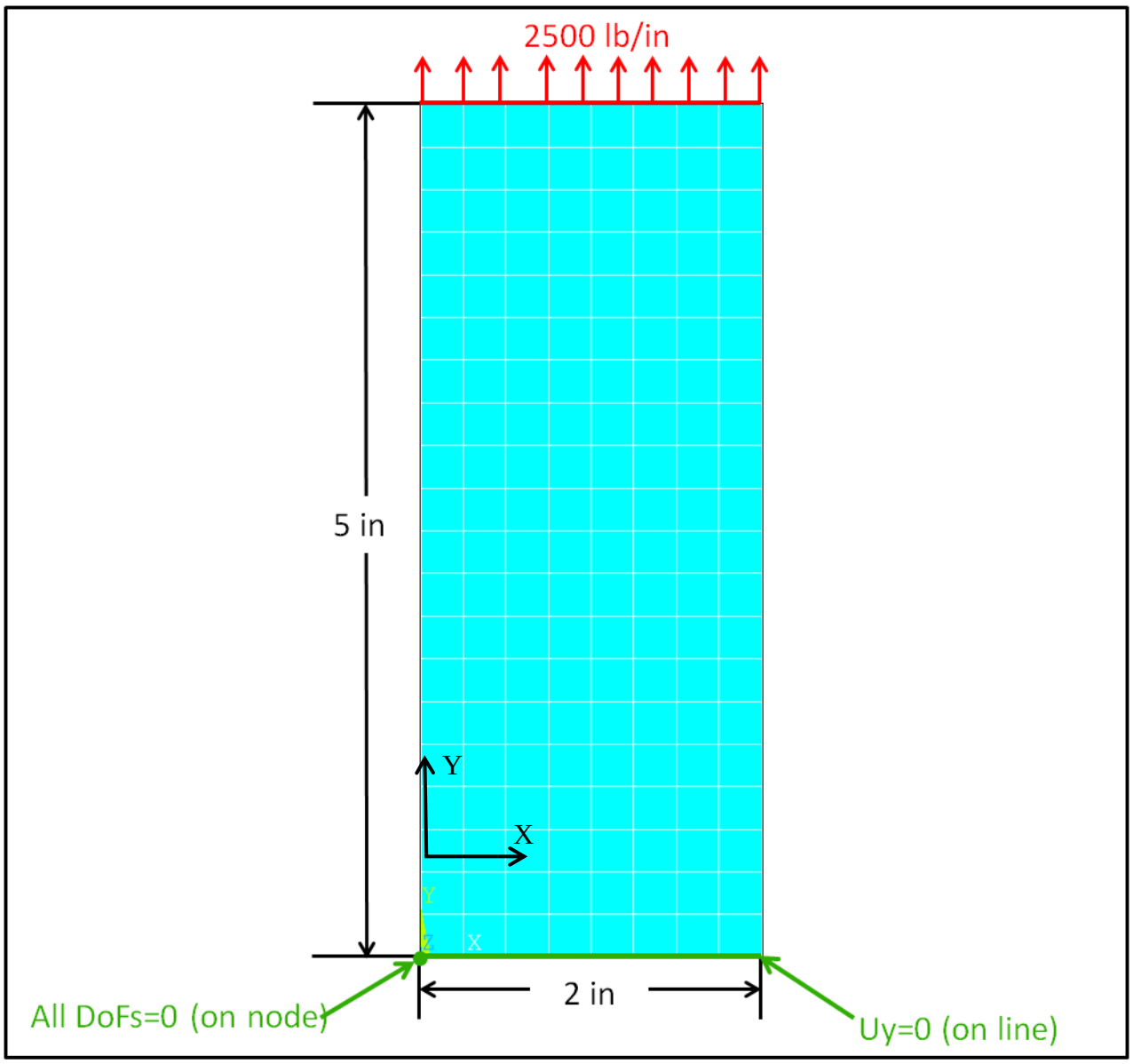

Figure 9: Mesh and applied boundary conditions

4 Simulation Results

The results discussed in this section were obtained by solving the model shown in Figure 9. The solutions will be divided into sections based on how they were obtained. The final section of this chapter will discuss a summary of the results obtained by FEA and theory.

4.1 ANSYS Results

The results discussed in this section were obtained by building the model discussed in chapter 3 in ANSYS. Stresses present in each layer of the laminate are displayed in tabular format throughout this section. Stresses in the unidirectional lay-up are listed in Table 5, stresses in the quasi-isotropic lay-up are listed in Table 6, and the stresses in the cross-ply lay-up are listed in Table 7.

Table 5: ANSYS stress results throughout each ply of a unidirectional layup

Unidirectional			
Layer number	**Stress X (psi)**	**Stress Y (psi)**	**Stress XY (psi)**
One	0	71429	0
Two	0	71429	0
Three	0	71429	0
Four	0	71429	0
Five	0	71429	0
Six	0	71429	0
Seven	0	71429	0

Table 6: ANSYS stress results throughout each ply of a quasi-isotropic layup

Quasi-isotropic			
Layer number	**Stress X psi**	**Stress Y psi**	**Stress XY psi**
One	-64531	17509	0
Two	32285	58885	36870
Three	32285	58885	-36870
Four	-79.242	229440	0
Five	32285	58885	-36870
Six	32285	58885	36870
Seven	-64531	17509	0

Table 7: ANSYS stress results throughout each ply of a cross-ply layup

Cross-ply			
Layer number	**Stress X psi**	**Stress Y psi**	**Stress XY psi**
One	-2432	12372	0
Two	3242	150170	0
Three	-2432	12372	0
Four	3242	150170	0
Five	-2432	12372	0
Six	3242	150170	0
Seven	-2432	12372	0

4.2 Abaqus Results

Initially results given by Abaqus appeared to be vastly different from the results given by ANSYS. After more investigation it was discovered that the results from ANSYS were output as stresses in the global coordinate directions of each ply and the results output by Abaqus were in the local directions of each ply. These differences were most apparent in the case of the quasi-

isotropic lay-up. Results directly from the Abaqus for the quasi-isotropic lay-up can be seen in Table 8.

Table 8: Abaqus stress results throughout each ply of a quasi-isotropic layup (shown in the principal directions)

Quasi-isotropic			
Layer number	**Stress 1 psi**	**Stress 2 psi**	**Stress 12 psi**
One	-64531	17509	0
Two	82456	8715	13300
Three	82456	8715	-13300
Four	229442	79	0
Five	82456	8715	-13300
Six	82456	8715	13300
Seven	-64531	17509	0

Results given by Abaqus were then transformed into the global coordinate system so that they could be compared with the ANSYS solutions. To do so a simple transformation was done. This transformation is described by the equations below.

$$\begin{Bmatrix} \sigma_x \\ \sigma_y \\ \sigma_{xy} \end{Bmatrix} = \begin{bmatrix} m^2 & n^2 & 2mn \\ n^2 & m^2 & -2mn \\ -mn & mn & m^2 - n^2 \end{bmatrix}^{-1} \begin{Bmatrix} \sigma_1 \\ \sigma_2 \\ \sigma_{12} \end{Bmatrix}$$

Where

$$m = \cos\theta$$

$$n = \sin\theta$$

Global stresses for the quasi-isotropic layup were obtained by applying the transformation shown above to the data seen in Table 8. The global results for the quasi-isotropic lay-up can be seen in Table 9. The global results for the cross-ply and unidirectional lay-ups are then seen in Table 10 and Table 11. (The Matlab script used to perform these transformations can be found in Appendix A.)

Table 9: Abaqus stress results throughout each ply of a quasi-isotropic layup

Quasi-isotropic			
Layer number	**Stress X psi**	**Stress Y psi**	**Stress XY psi**
One	-64531	17509	0
Two	32285	58885	36870
Three	32285	58885	-36870
Four	-79.242	229440	0
Five	32285	58885	-36870
Six	32285	58885	36870
Seven	-64531	17509	0

The stresses obtained from Abaqus, after they were transformed, exactly match the stresses given by ANSYS. Therefore, when modeling laminates under static loads it does not matter if ANSYS or Abaqus is used. It may not matter what package is used but it is important to understand how to use each of them properly and to understand how results are output from each package.

Table 10: Abaqus stress results throughout each ply of a unidirectional layup

Unidirectional			
Layer number	**Stress X psi**	**Stress Y psi**	**Stress XY psi**
One	0	71429	0
Two	0	71429	0
Three	0	71429	0
Four	0	71429	0
Five	0	71429	0
Six	0	71429	0
Seven	0	71429	0

Table 11: Abaqus stress results throughout each ply of a cross-ply layup

Cross-ply			
Layer number	**Stress X psi**	**Stress Y psi**	**Stress XY psi**
One	-2432	12372	0
Two	3242	150170	0
Three	-2432	12372	0
Four	3242	150170	0
Five	-2432	12372	0
Six	3242	150170	0
Seven	-2432	12372	0

4.3 Theoretical Results

To verify the FEA solutions the theory discussed in chapter 2 was applied to the geometry and loading conditions shown in Figure 9. The results for the three different lay-ups of interest are listed in Table 12, Table 13, and Table 14. (The Matlab script used to calculate the theoretical results was provided by Brooks Marquette and can be found in Appendix B.)

Table 12: Theoretical stress results throughout each ply of a unidirectional layup

Unidirectional			
Layer number	**Stress X psi**	**Stress Y psi**	**Stress XY psi**
One	0	71429	0
Two	0	71429	0
Three	0	71429	0
Four	0	71429	0
Five	0	71429	0
Six	0	71429	0
Seven	0	71429	0

It is seen from the stresses listed in the tables throughout this section that theory matches solutions returned by FEA. This is important because it proves that the FEA solutions are accurate to laminate theory.

Table 13: Theoretical stress results throughout each ply of a quasi-isotropic layup

Quasi-isotropic			
Layer number	**Stress X psi**	**Stress Y psi**	**Stress XY psi**
One	-64531	17509	0
Two	32285	58885	36870
Three	32285	58885	-36870
Four	-79.242	229440	0
Five	32285	58885	-36870
Six	32285	58885	36870
Seven	-64531	17509	0

Table 14: Theoretical stress results throughout each ply of a cross-ply layup

Cross-ply			
Layer number	**Stress X psi**	**Stress Y psi**	**Stress XY psi**
One	-2432	12372	0
Two	3242	150170	0
Three	-2432	12372	0
Four	3242	150170	0
Five	-2432	12372	0
Six	3242	150170	0
Seven	-2432	12372	0

4.4 Results Summary

The results shown throughout the previous three sections of this chapter were reduced to three plots of the stresses through the thickness of the laminate. A plot of the stress through a unidirectional layup is seen in Figure 10.

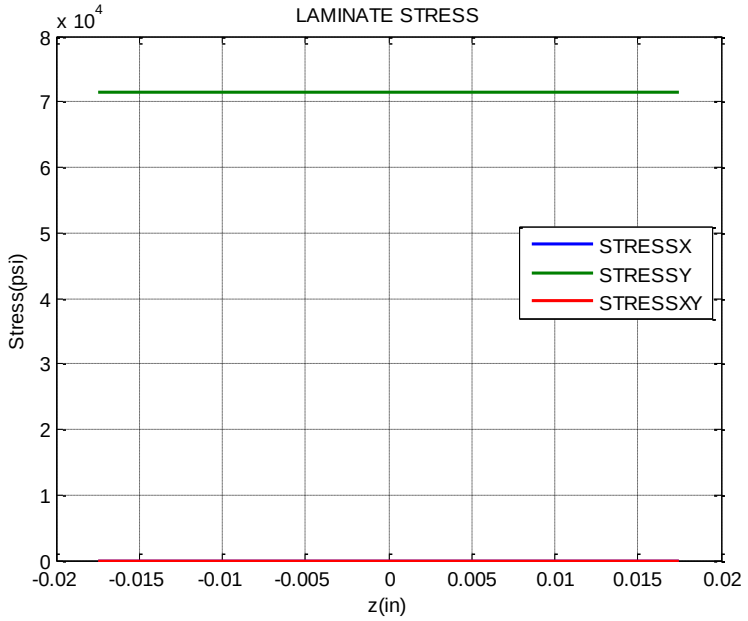

Figure 10: Stresses through the thickness of a unidirectional layup

Figure 10 shows that the only stress present throughout the unidirectional lay-up is in the y direction. Stress only exists in the y direction because each layer is oriented perpendicular to the direction of loading. This would also be true if the all of the layers were oriented parallel to the direction of loading. For the tension tests discussed in this document, the only time that stress will simultaneously be present in the x, y, and xy directions will be in the multi-directional layups. The plot of the stress through the thickness of a quasi-isotropic lay-up can be seen in Figure 11 and for a cross-ply this plot is seen in Figure 12.

Shear and lateral stresses will never exist in any type of unidirectional layup where the loading is parallel or perpendicular to the fiber directions. This is seen mathematically in the $[\bar{Q}]$ matrix. If the fibers are oriented at 0 or 90 degrees the shear terms, $\bar{Q}_{16}$ and $\bar{Q}_{26}$, go to zero. Any other case where the fibers aren't parallel or perpendicular to the loading direction the shear terms wouldn't be zero; therefore, there will be shear stresses through the part.

The stresses throughout the thickness of a quasi-isotropic lay-up are much more interesting than the stresses through a unidirectional lay-up. As is seen in Figure 11, the stress in the y direction of the center ply is much higher than any of the other plies. This is expected because the center ply is oriented with the fibers parallel to the direction of loading. Since strains are considered to be equal in every ply and the center ply is has the highest stiffness in the direction of loading, the center ply should therefore have the highest stress. Figure 11 also shows that the stresses in ply 1 are equal to stresses in ply 7, stresses in ply 2 are equal to stresses in ply 6, and stresses in ply 3 are equal to stresses in ply 5. This symmetry condition can be applied to simplify each of the models. The same symmetry condition is shown by the unidirectional and cross-ply lay-ups.

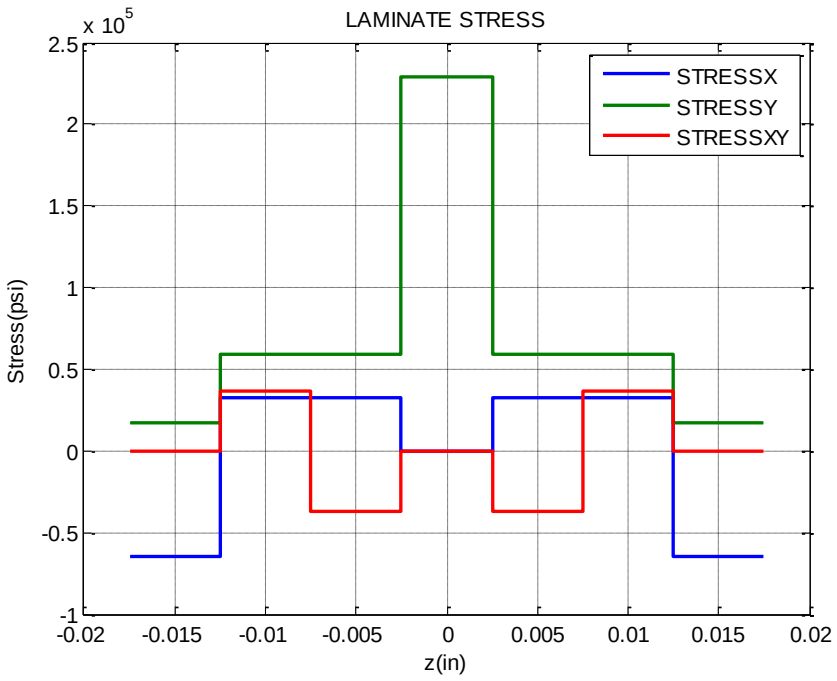

Figure 11: Stresses through the thickness of a quasi-isotropic layup

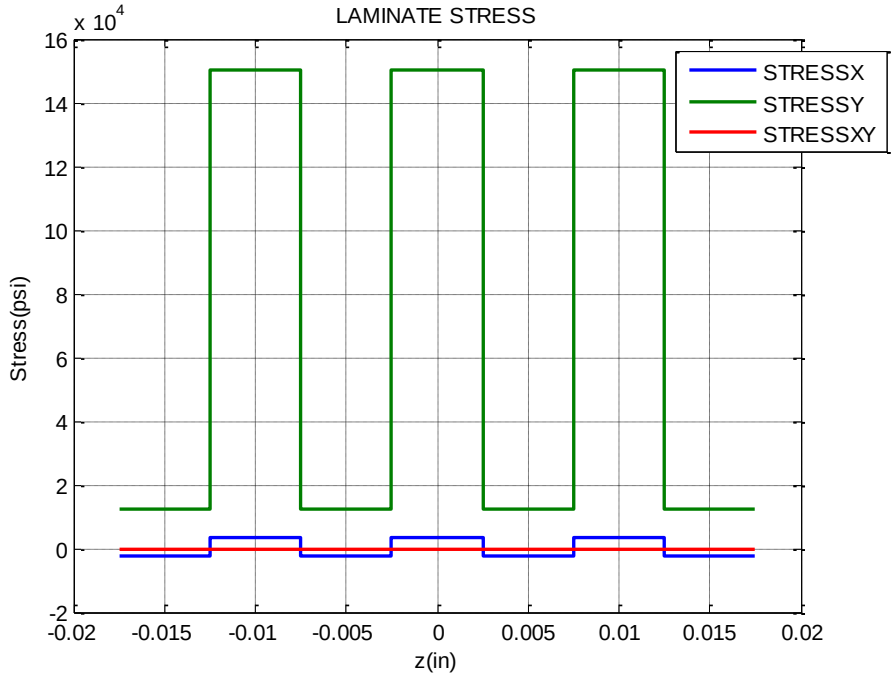

Figure 12: Stresses through the thickness of a cross-ply layup

The stresses seen throughout the thickness of the cross-ply lay-up are also expected. Since the fiber orientations alternate back and forth between being perpendicular and parallel with the direction of loading, it is expected the stress in the y direction should go from low to high because of the large variation of the stiffness in the direction of loading. It is also seen that the stress in the xy direction is also zero. This is because the direction of loading is always parallel to a principal direction of a respective ply.

The average stress throughout the thickness of a respective lay-up can also be used to further verify the results. The following equation can be used to check the average stress.

$$\sigma_y = \frac{F}{A}$$

Where, in the case of this simulation

$$F = 5000\ lbs$$

$$A = 2 * 0.005 * 7 = 0.07\ in^2$$

Therefore,

$$\sigma_y = 71429\ psi$$

The stress value shown is equal to the average stress in the y direction throughout each respective laminate. The average stresses in the y-direction for each lay-up are shown in Table 15

Table 15: Average stress comparison

Average Stress in the y-direction		
Unidirectional	**Quasi-isotropic**	**Cross-ply**
71429 psi	71429 psi	71429 psi

As is seen in the above table, the average stress for each lay-up is equal to 71429 psi. It is also important to note that the stresses in the x and xy directions average to zero for each lay-up.

5 Application of FEA to complex geometries

Since the finite element code has been proved to be accurate to theory it is plausible to begin solving tension tests of more complex geometries. Two more complex geometries are shown throughout this chapter; they are a holed specimen and a notched specimen.

5.1 Hole tension test

The holed specimen modeled in this section has the same dimensions, constraints, and load as the model discussed in chapter 3. The only differences are, an element edge sizing of 0.05, and a one inch diameter hole drilled through its center. The lay-up for this test was selected as quasi-isotropic. An image of the mesh used in ANSYS is shown in Figure 13.

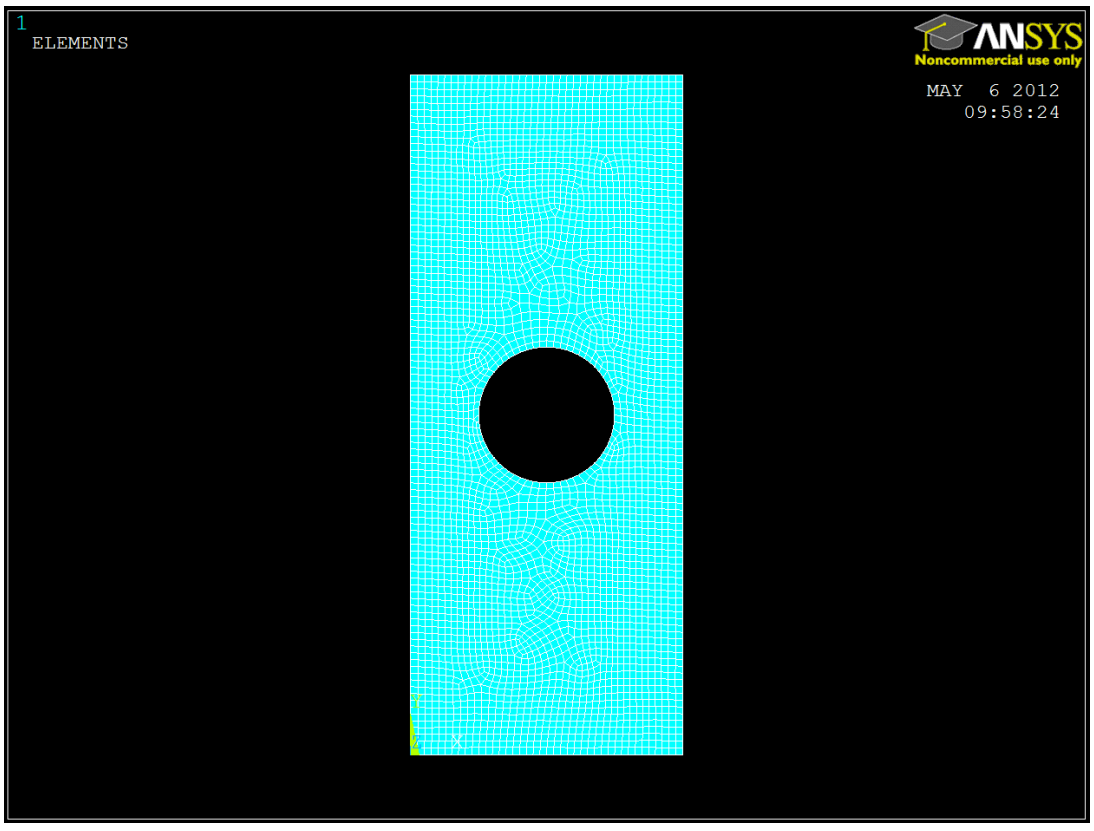

Figure 13: Mesh used for the tension simulation of a holed specimen

Solutions for the stresses in the y direction are shown in the following figures. To simplify the problem some of the previously discussed symmetry conditions were accounted for. Therefore, the stresses in layers one and seven are shown in Figure 14, stresses in layers two and six are shown in Figure 15, stresses in layers three and five are shown in Figure 16, and the stresses in layer four are shown in Figure 17. The discontinuity in the material causes the stresses to vary greatly at all locations throughout a single ply. (All contour plots show the stresses as psi.)

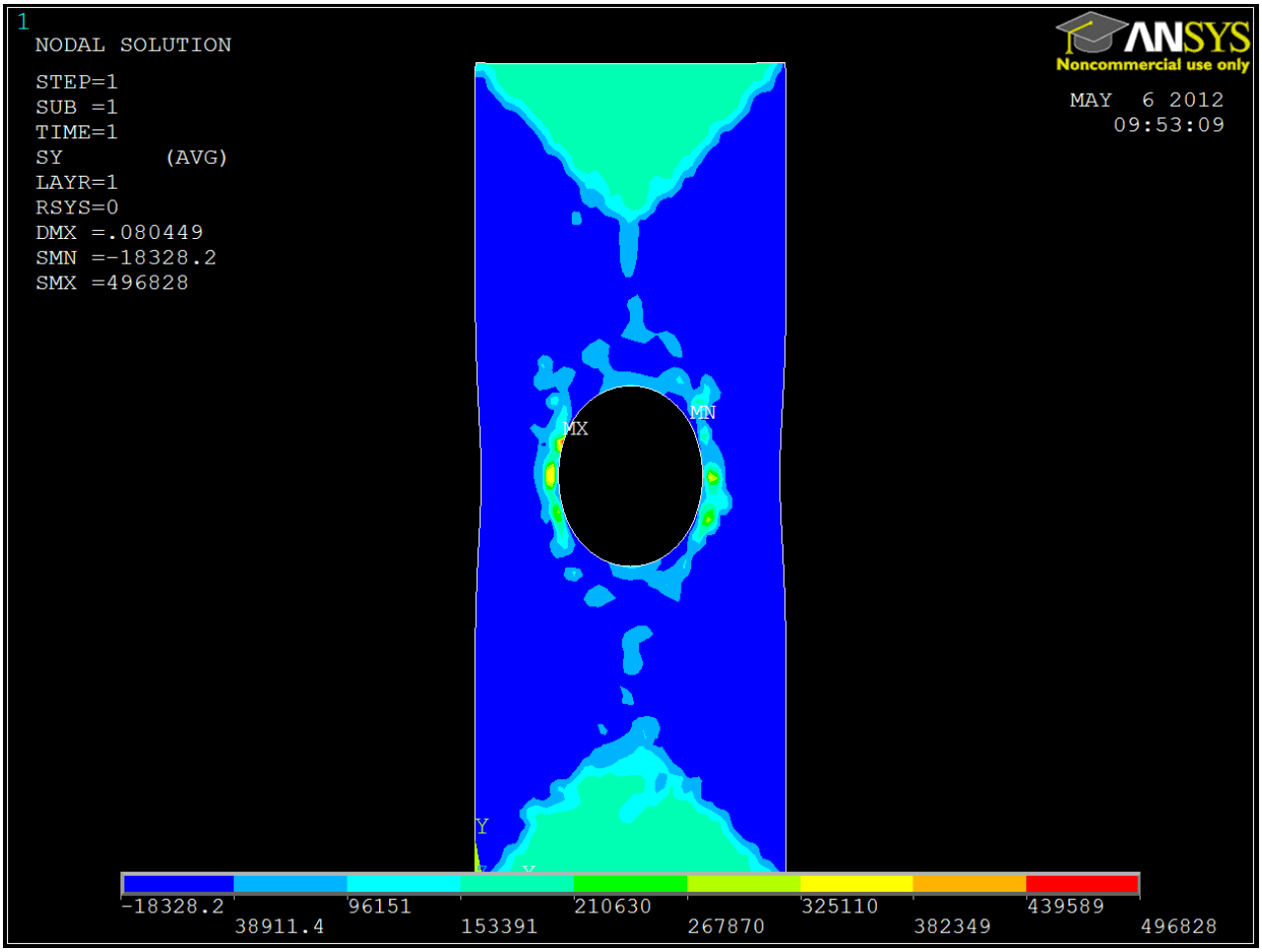

Figure 14: Stress in the y direction in layers 1 and 7 of a holed specimen in tension

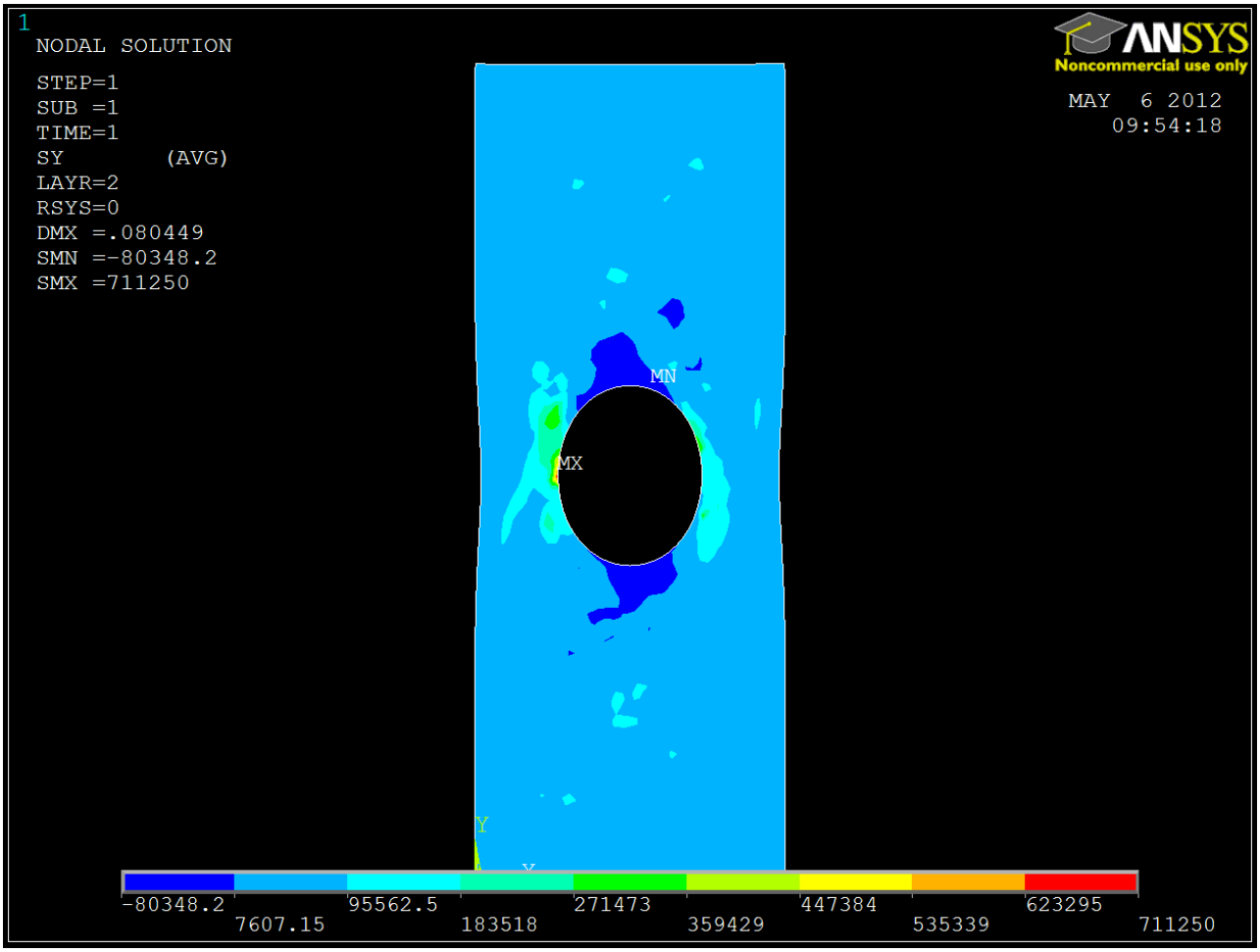

Figure 15: Stress in the y direction in layers 2 and 6 of a holed specimen in tension

The contour plots shown for each layer of the holed specimen display some peculiar behaviors. In the unidirectional ply shown in Figure 14 it is seen that there are triangular shaped regions near the constrained and loaded edges. These triangular regions contain an average stress between 150 ksi and 200 ksi. Outside of these regions the stress then drops to -18 ksi until it begins to increase again in the presence of the hole. Figure 14 can then be compared to Figure 17, which is the 90 degree ply. The 90 degree ply also shows triangular contours at the loaded and constrained edges. Only in these triangles the stress is lower than the regions directly outside of the triangle. The contour shapes in Figure 14 and Figure 17 show similar trends, but

the contours are inverted as far as their relative magnitudes. This should be expected since the first ply is loaded perpendicular to the fiber direction and the fourth ply is loaded parallel to the fiber direction. The material has the lowest stiffness in the direction perpendicular to the fibers and the highest stiffness parallel to the fibers. It is also seen, in Figure 15 and Figure 16, that the 45 degree and -45 degree ply tend to transfer the stress at an angle. This should also be expected because the orthotropic material properties.

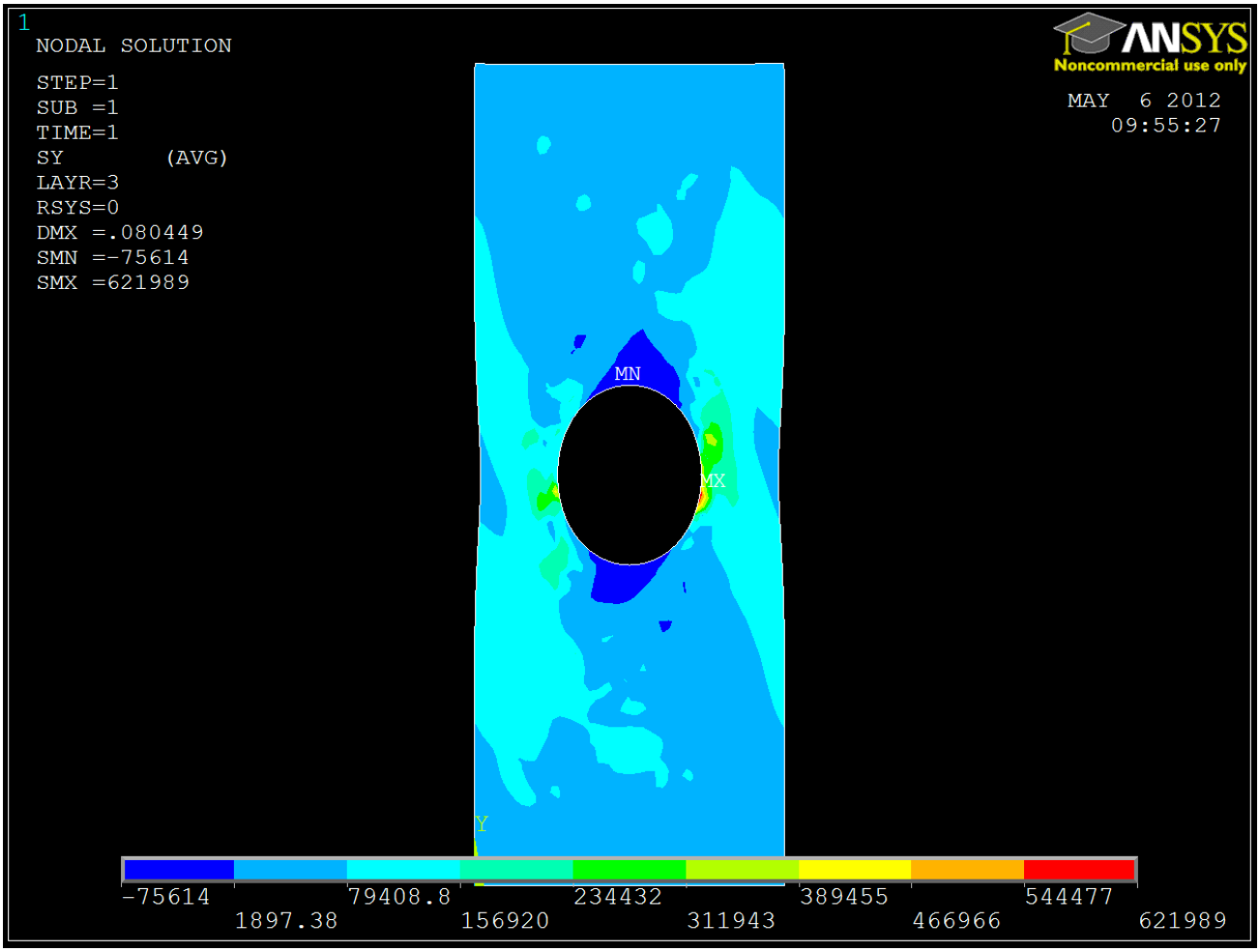

Figure 16: Stress in the y direction in layers 3 and 5 of a holed specimen in tension

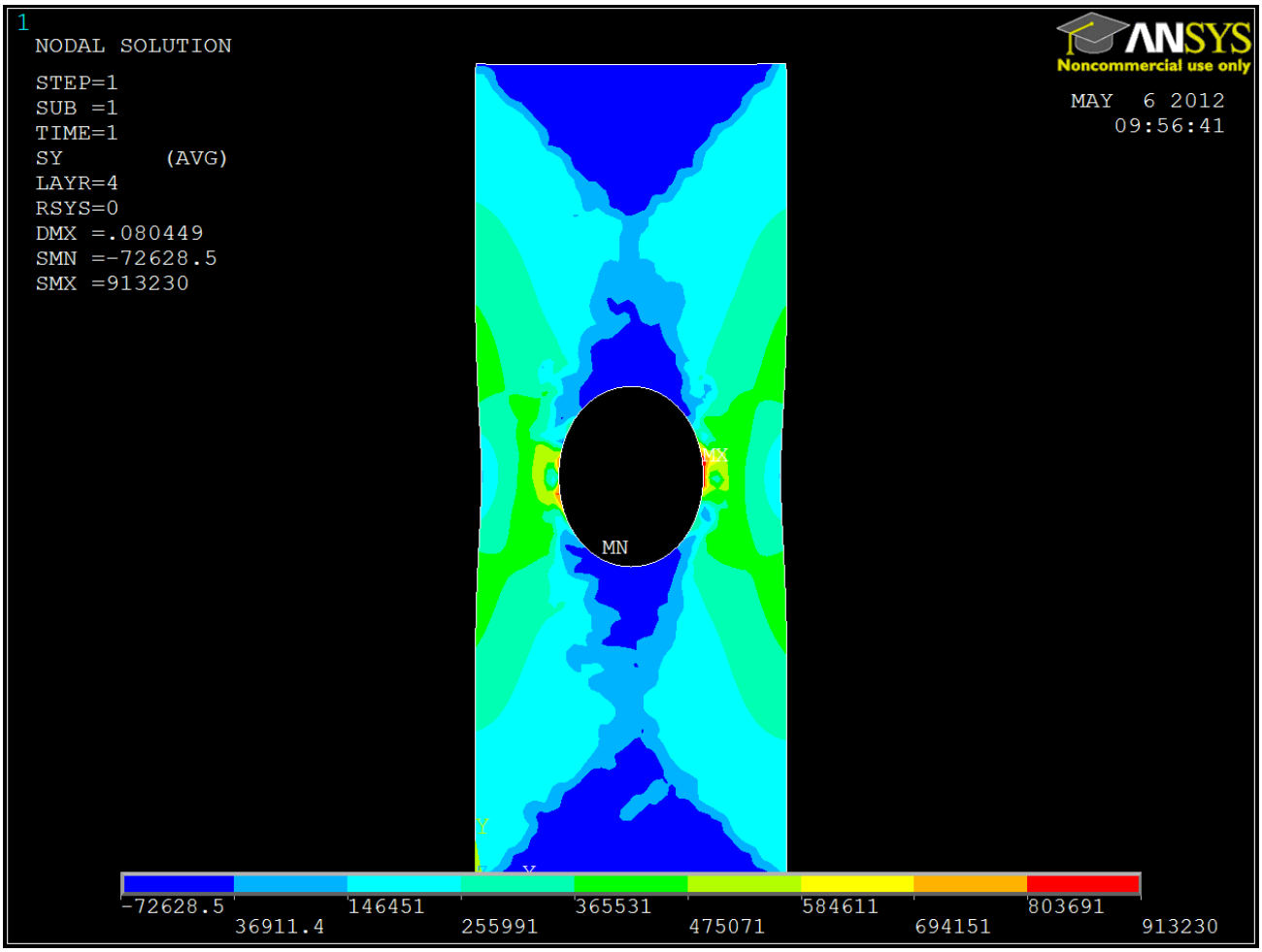

Figure 17: Stress in the y direction in layer 4 of a holed specimen in tension

5.2 Notch tension test

The notched specimen modeled in this section has the same dimensions, constraints, and load as the model discussed in chapter 3. The only differences are, an element edge sizing of 0.05, and two notches cut out of each side of the specimen. The lay-up for this test was selected as quasi-isotropic. An image of the mesh used in ANSYS is shown in Figure 18.

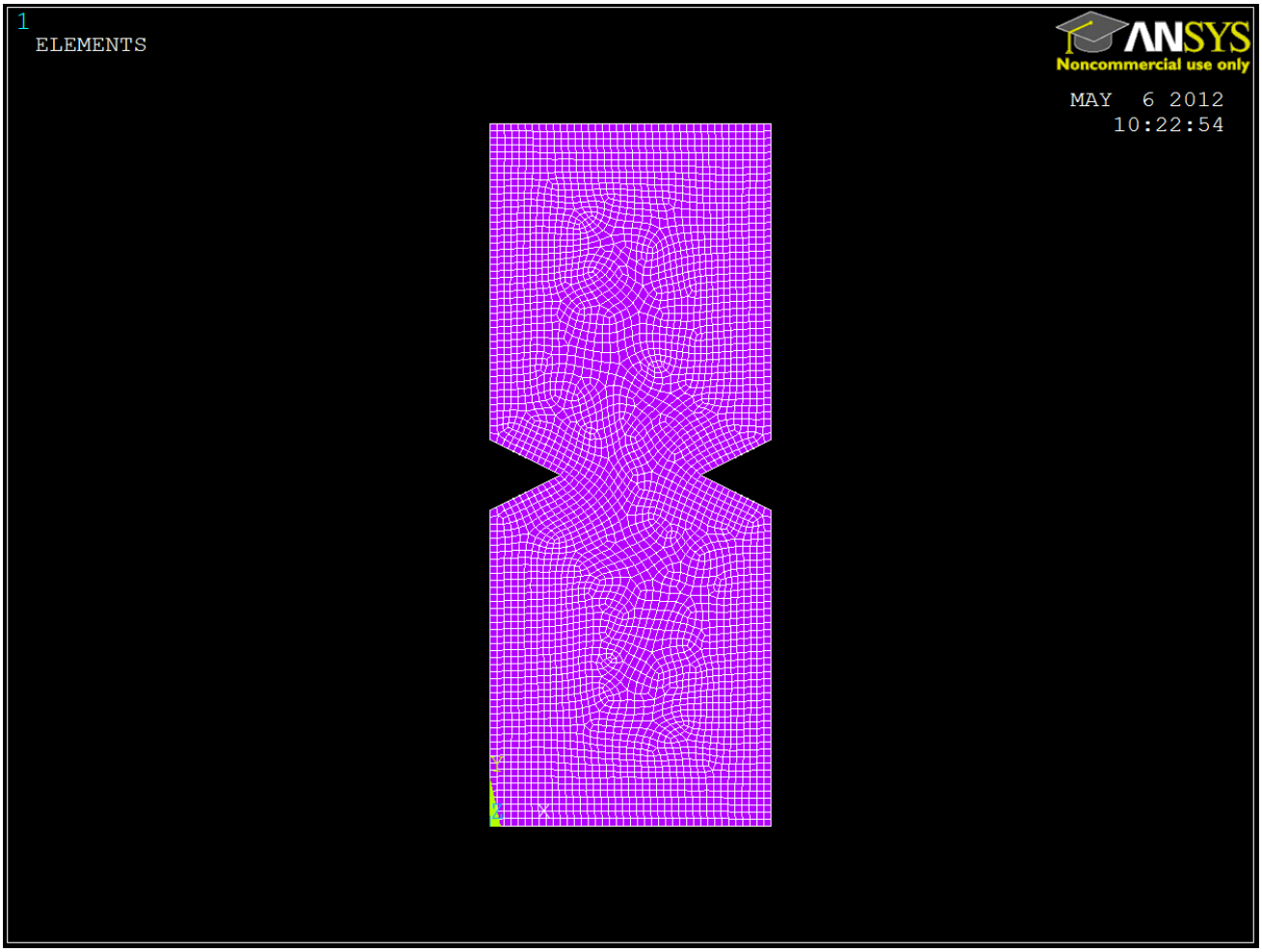

Figure 18: Mesh used for the tension simulation of a notched specimen

Solutions for the stresses in the y direction are shown in the following figures. To simplify the problem the previously discussed symmetry conditions were accounted for. Therefore, the stresses in layers one and seven are shown in Figure 19, stresses in layers two and six are shown in Figure 20, stresses in layers three and five are shown in Figure 21, and the stresses in layer four are shown in Figure 22. The discontinuity in the material causes the stresses to vary greatly at all locations throughout a single ply.

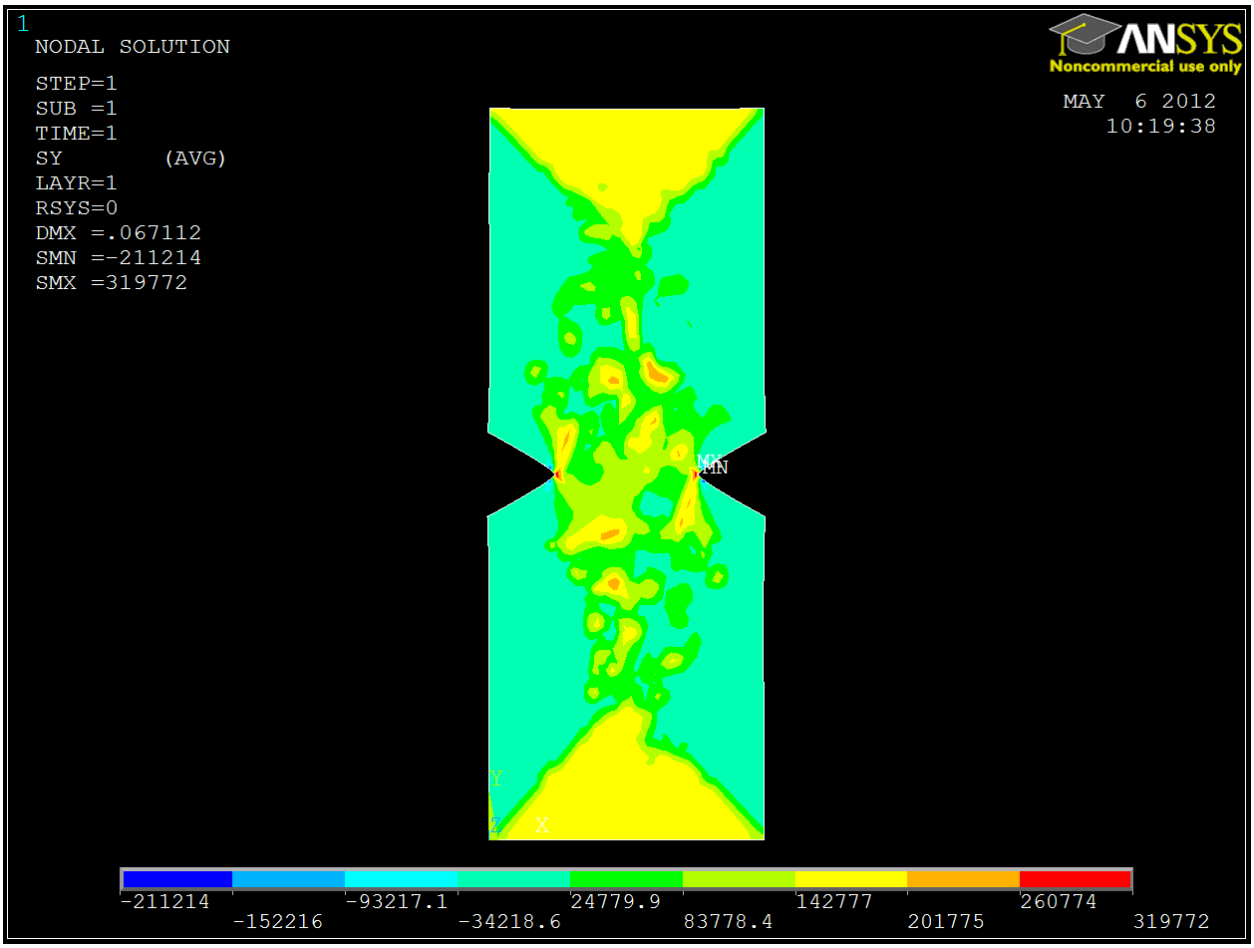

Figure 19: Stress in the y direction in layers 1 and 7 of a notched specimen in tension

In the case of the notched specimen it is also important to note that the stress concentration at the point of the notch is artificial. This is because in reality there is no such thing as perfectly sharp edge, which is what the FEA software sees the notch point as. To combat this problem, in the future, a slight radius will be added to the notch point. With the added radius the mesh will also be refined in the region of the notch in order to capture the high stress gradient that is occurring in this region. With mesh refinement an artificial stress concentration may still be present. Its presence will be obvious because the stress magnitude will trend to infinity as the mesh becomes finer. If this is the case the surrounding stress values should be used as the maximum stress.

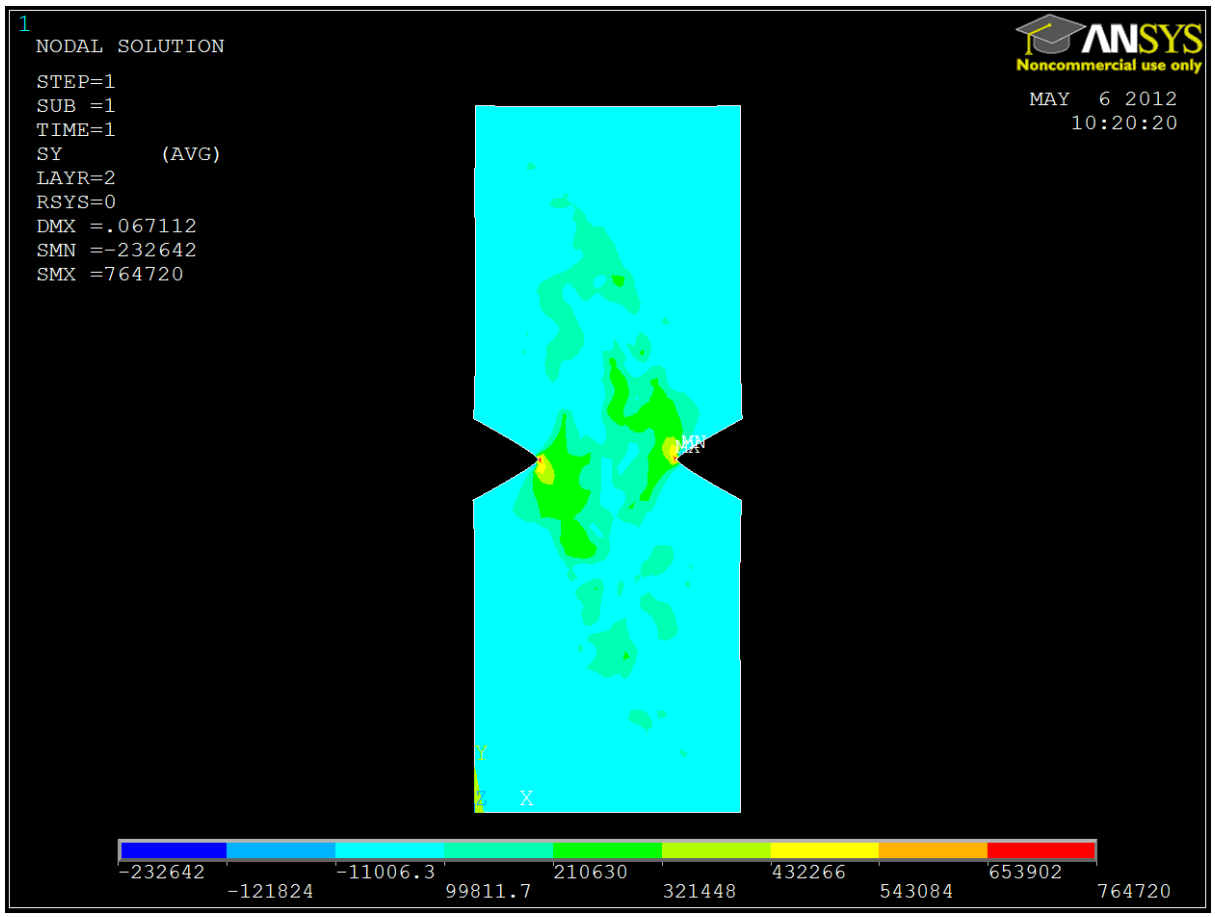

Figure 20: Stress in the y direction in layers 2 and 6 of a notched specimen in tension

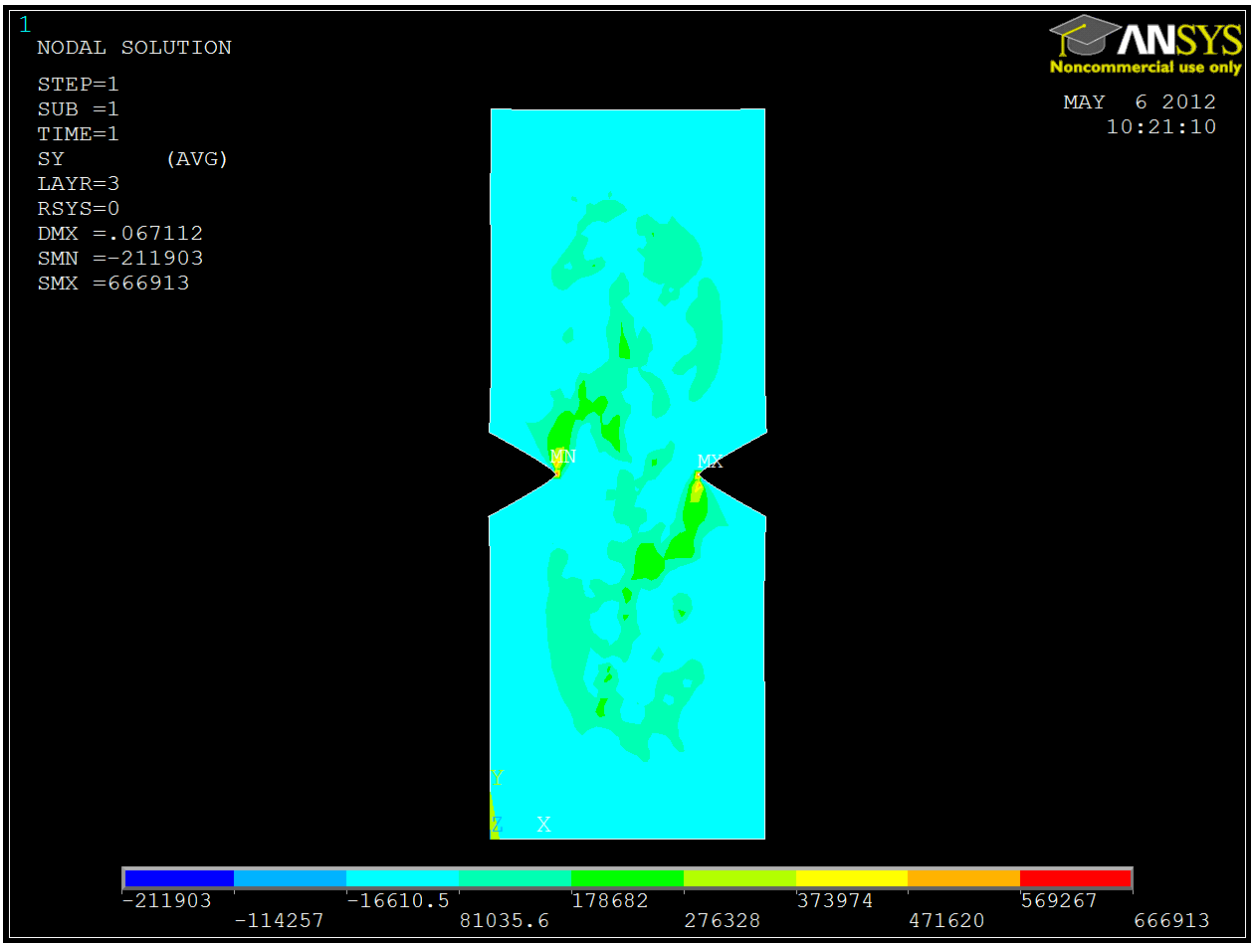

Figure 21: Stress in the y direction in layers 3 and 5 of a notched specimen in tension

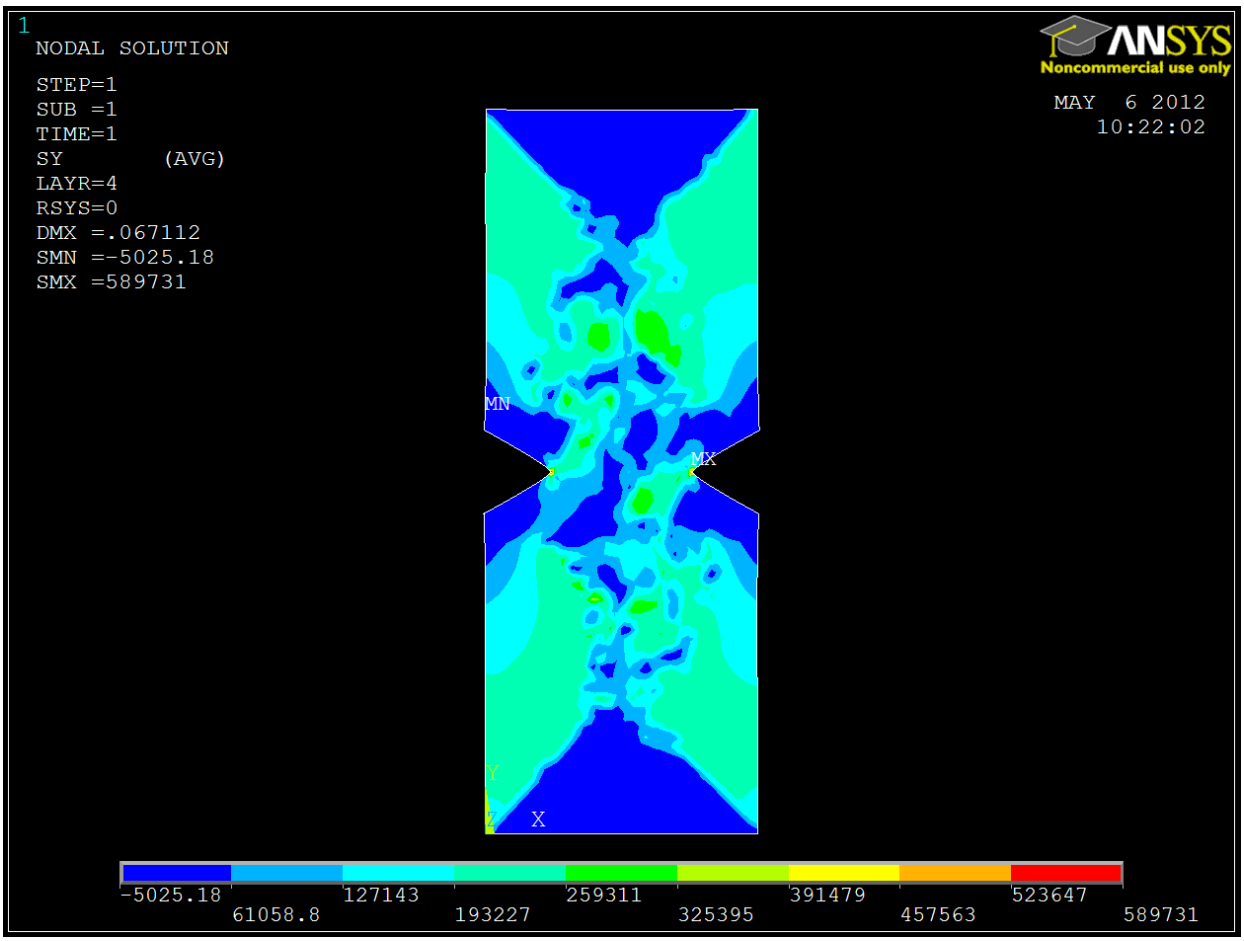

Figure 22: Stress in the y direction in layer 4 of a notched specimen in tension

6 Conclusions

The purpose of the research discussed throughout this thesis was to investigate and determine the composite modeling capabilities of commercial FEA software. The selected software packages were ANSYS and Abaqus, chosen because of their availability at The Ohio State University. The research provided insight on the mechanical responses orthotropic material and how to properly construct FEA models of CFRPs in each of the aforementioned software packages.

6.1 Contributions

This research will help add to the knowledge base of FEA of composite materials. It proves that FEA is accurate to current laminate theory and the results are independent of the software package used to obtain them. Therefore, only one software package can be selected based on ease of use instead of its accuracy.

6.2 Additional Applications

The approach discussed for modeling composites is applicable to many situations. It could be applied to geometries like the ones discussed in chapter 5. This approach is also not limited to tension tests. Samples that under go transverse loads can also be modeled quite easily using these methods.

Three dimensional parts can also be modeled using shell sections. For example the shell sections can be applied to an airplane fuselage, a wing, body panels on automobiles, automobile hoods, etc. As long as the part is thin enough it can be meshed using shells.

6.3 Future Work

Modeling composite materials is more difficult than modeling traditional materials. Therefore, predicting the point at which a CFRP will fail is also more difficult. ANSYS and Abaqus do have built in failure theories that can be used with the shell sections, but they will not show any detail about the failure. For example, one type of failure of a composite laminate is known as delamination. Delamination occurs when the plies of the laminate begin to separate from each other. Shell sections would not be able to accurately predict this type of failure because they are not detailed enough to show how the plies will interact with each other. To model this type of failure another method must be used. Since part of the future work will be predicting a failure of a CFRP it will be important to learn how to model delamination.

Knowledge gained form this project will also be used to create models that attempt to match experimental tests. Matching experimental test results would help further validate FEA and help develop more accurate techniques of modeling composites. This knowledge could then be used to optimize the design process of composite parts.

6.4 Summary

This project has investigated and compared the modeling capabilities of ANSYS and Abaqus, compared the mechanical reactions of three different lay-up patterns, and verified all of this with current laminate theory. Following verification the discussed techniques were applied to simulate tension tests of a holed and notched specimen. The modeling techniques discussed throughout this document increase the knowledge base of modeling composite materials and can be implemented to help verify experimental tests and design parts for aircraft or automobiles.

Appendix A

```
clc
clear all
close all
format long
%%%%%%%%%%%%%%%%%%%%%%%%%%%%%%%%%%%%%%%%%%%%%%%%%%%%%%%%%%%%%%%%%%%%%%%%%%%%%%%%%%%
%laminate information
%theta=[0;0;0;0;0;0;0];%uni-directional
theta=[0;45;-45;90;-45;45;0];%quasi-isotropic
%theta=[0;90;0;90;0;90;0];%cross-ply
ply_thickness=0.005;
number_of_plys=length(theta);
ply_thickness=ply_thickness*ones(number_of_plys,1);
width=2;
%material properties
E_1=18e6;
E_2=1.5e6;
G_12=0.8e6;
v_12=0.3;
%loading
N=[0;5000;0]/width;
M=[0;0;0]/width;
%Maximum tensile stress values
X=2723e6;
Y=111e6;
S=68e6;
%%%%%%%%%%%%%%%%%%%%%%%%%%%%%%%%%%%%%%%%%%%%%%%%%%%%%%%%%%%%%%%%%%%%%%%%%%%%%%%%%%%
%creating the Q matrix
v_21=E_2*v_12/E_1;
Q11=E_1/(1-v_12*v_21);
Q22=E_2/(1-v_12*v_21);
Q12=v_12*E_2/(1-v_12*v_21);
Q66=G_12;
Q=[Q11,Q12,0;Q12,Q22,0;0,0,Q66];
m=cosd(theta);
n=sind(theta);
h=sum(ply_thickness);
A=zeros(3,3);
B=zeros(3,3);
D=zeros(3,3);
z(1,:)=(-h/2)+ply_thickness(1)/2;
for i=2:number_of_plys
    z(i,:)=z(i-1)+ply_thickness(i-1)/2+ply_thickness(i)/2;
end
for i=1:number_of_plys

    T_strain(:,:,i)=[m(i)^2,n(i)^2,m(i)*n(i);
                     n(i)^2,m(i)^2,-m(i)*n(i);
                    -2*m(i)*n(i),2*m(i)*n(i),m(i)^2-n(i)^2];

    T_stress(:,:,i)=[m(i)^2,n(i)^2,2*m(i)*n(i);
                     n(i)^2,m(i)^2,-2*m(i)*n(i);
```

```
                    -m(i)*n(i),m(i)*n(i),m(i)^2-n(i)^2];

    Q_bar(:,:,i)=inv(T_stress(:,:,i))*Q*T_strain(:,:,i);

    A=A+Q_bar(:,:,i)*ply_thickness(i);
    B=B+Q_bar(:,:,i)*(ply_thickness(i)*z(i));
    D=D+Q_bar(:,:,i)*(ply_thickness(i)*z(i)^2+ply_thickness(i)^3/12);

end
STRAIN=inv(A)*N;
KAPPA=inv(D)*M;
for i=1:number_of_plys
    sig_g(:,i)=Q_bar(:,:,i)*STRAIN;
    sig_p(:,i)=T_stress(:,:,i)*sig_g(:,i);
end
```

Appendix B

```
%Undergraduate Thesis
%Code Provided By Brooks Marquette
%Modified by Brice Willis
%7 ply tesion test
%uni-directional
clc
clear all
close all
%inputs start
%please enter the following values specific to the lamina of interest
tply=0.005; %ply thickness
Plynumber=7;%number of plys
tply=tply*ones(Plynumber,1);%Will need to specify individual plies if
different thickness
%enter the orientation of each ply in order from 1 to n
%theta=[90;90;90;90;90;90;90];
%theta=[0;0;0;0;0;0;0]*pi/180;%uni-directional
theta=[0;45;-45;90;-45;45;0]*pi/180;%quasi-isotropic
%theta=[0;90;0;90;0;90;0]*pi/180;%cross-ply
%elastic parameters taken from Feraboli
E1=18e6;
E2=1.5e6;
G12=0.8e6;
%Vf=0.7;
v12=0.3;
v21=E2*v12/E1;
w=2; %Width of sample
N=[0;5000;0]/w; %Tensile applied Stess
M=[0;0;0]/w; %Bending Moment Stress
%inputs end

h=sum(tply);
A=zeros(3,3);
B=zeros(3,3);
D=zeros(3,3);

for i=1:Plynumber
 m=cos(theta(i));
 n=sin(theta(i));

 z(1,:)=(-h/2)+tply(1)/2;
  if i>=2
     z(i,:)=z(i-1)+tply(i-1)/2+tply(i)/2;
  end

 % To create Q Bar matrix and ABD matrix

Q11=E1/(1-v12*v21);
Q22=E2/(1-v12*v21);
Q12=v12*E2/(1-v12*v21);
Q66=G12;
```

```
Q11_=Q11*m^4+2*(Q12+2*Q66)*m^2*n^2+Q22*n^4;
Q12_=(Q11+Q22-4*Q66)*m^2*n^2+Q12*(m^4+n^4);
Q22_=Q11*n^4+2*(Q12+2*Q66)*m^2*n^2+Q22*m^4;
Q16_=-Q22*m*n^3+Q11*m^3*n-(Q12+2*Q66)*m*n*(m^2-n^2);
Q26_=-Q22*n*m^3+Q11*n^3*m-(Q12+2*Q66)*m*n*(m^2-n^2);
Q66_=(Q11+Q22-2*Q12)*m^2*n^2+Q66*(m^2-n^2)^2;
Q_(:,:,i)=[Q11_,Q12_,Q16_;Q12_,Q22_,Q26_;Q16_,Q26_,Q66_];

A=A+Q_(:,:,i)*(tply(i));
B=B+Q_(:,:,i)*(tply(i)*z(i));
D=D+Q_(:,:,i)*(tply(i)*z(i)^2+tply(i)^3/12);
end
Aa=inv(A);
Dd=inv(D);
STRAIN=Aa*N;
KAPPA=Dd*M;
for i=1:Plynumber*2

    if rem(i/2,1)>0
        zout(i)=z(round(i/2))-tply(round(i/2))/2;
    else
        zout(i)=z(round(i/2))+tply(round(i/2))/2;
    end
    STRESS(:,i)=Q_(:,:,round(i/2))*(STRAIN+zout(i)*KAPPA);

end

figure(1)
plot(zout,STRESS,'linewidth',2)
title('LAMINATE STRESS')
xlabel('z(in)')
ylabel('Stress(psi)')
grid on
legend('STRESSX','STRESSY','STRESSXY')
```

References

Anonymous. (2008). Abaqus/CAE User's Manual. Providence, RI, USA.

Anonymous_2. (2009). ANSYS Help System version 12.0. Canonsburg, PA, USA: ANSYS.

Ashby, M. F. (2005). *Materials Selection in Mechanical Design.* Burlington: Elsevier.

Feraboli, P., & Kedward, K. T. (2003). Four-point bend interlaminar shear testing of uni- and multi-directional carbon/epoxy composite systems. *Composites: Part A*.

Miracle, D. B., & Donaldson, S. L. (2001). ASM Handbook, Volume 21-Composites. In D. B. Miracle, & S. L. Donaldson, *ASM Handbook, Volume 21-Composites.* ASM International.

Staab, G. H. (1999). *Laminar Composites.* Woburn: Butterworth-Heinemann.

Swanson, S. R. (1997). *Introduction to Design and Analysis with Advanced Composite Materials.* Upper Saddle River: Simon & Schuster.

Unknown. (2008). *Why Carbon Fiber*. Retrieved March 2012, from Plasan Carbon Composites: http://www.plasancarbon.com/template/default.aspx?catid=2&PageId=18